MINISTRY OF EDUCATION AND RESEARCH
TECHNICAL UNIVERSITY OF CIVIL ENGINEERING BUCHAREST
FACULTY OF RAILWAYS, ROADS AND BRIDGES

DOCTORAL THESIS
Summary

PhD. Candidate
Eng. Șimon Vlad-Mihai

STUDY OF THE DYNAMIC RESPONSE OF BRIDGES EQUIPPED WITH SEISMIC PROTECTION DEVICES

Scientific Supervisor
Prof. Dr. Eng. Răcănel Ionuț Radu

BUCHAREST 2026

TABLE OF CONTENTS

Chapter 1. INTRODUCTION AND GENERAL CONTEXT

1.1 Seismic context of Romania

Romania is among the European countries with the highest seismic risk, mainly due to the presence of the Vrancea seismogenic area, a globally unique seismic source capable of producing major earthquakes with magnitudes between 7 and 8 (1802: $M_w = 7.90$; 1940: $M_w = 7.70$; 1977: $M_w = 7.40$) within a restricted seismogenic volume, at intermediate depths of 60-180 km [1]. The event of 4 March 1977 remains the most significant earthquake recorded in Romania in the instrumental era and has served as the reference point for calibrating seismic hazard models.

Romania's road infrastructure includes a significant number of bridges built between 1960 and 1990, designed according to standards of the time that did not impose explicit ductility requirements or seismic isolation systems. The combination of historical structural deficiencies and current seismic risks creates a major vulnerability, as highlighted by international experiences from the Loma Prieta (1989), Northridge (1994), and Kobe (1995) earthquakes.

1.2 Research motivation

Elastomeric bearings represent the most commonly used solution for road bridges in Romania. Designed primarily for service conditions (thermal variations, permanent loads), they are not intended to accommodate seismic displacements associated with earthquakes with return periods exceeding the design value. International experience has shown that bearing failure, followed by loss of deck support, is one of the most frequent bridge damage mechanisms.

In this context, a comparative assessment of the seismic performance of bridges with various bearing systems, from conventional to advanced seismic isolation, represents a necessity for Romanian infrastructure.

1.3 Objective of the Thesis

The main objective of this doctoral thesis is the comparative assessment of the dynamic response of continuous girder prestressed concrete bridges equipped with four bearing systems: neoprene elastomeric bearings, pot bearings, Lead Rubber Bearings (LRB), and Friction Pendulum System (FPS) isolators. The main objectives are:

1. Assessment of seismic performance using nonlinear static Pushover analysis and the MADRS equivalent linearization procedure from FEMA 440 [2], with determination of behavior factors (q) for all bearing systems;
2. Quantification of seismic response reduction using isolation systems versus conventional bearings, based on 560 nonlinear Time-History dynamic analyses with direct integration;

3. Construction of IDA curves and fragility curves for non-isolated structures, with determination of non-exceedance probabilities for IO, LS, and CP performance levels per FEMA 356 [3];
4. Establishment of a practical correlation between the behavior factor q and the non-exceedance probability P%, as a rapid seismic vulnerability estimation tool;
5. Formulation of practical recommendations regarding the choice of optimal bearing system in high seismicity zones, specific to Romanian conditions.

1.4 Structure of the Thesis

The work is organized into seven chapters. Chapter 1 presents Romania's seismic context and research motivation. Chapter 2 analyses the historical effects of major earthquakes on bridges and the need for seismic isolation. Chapter 3 describes the evolution of seismic design codes. Chapter 4 presents the main types of seismic isolation devices. Chapter 5 details methodologies for assessing bridge seismic vulnerability. Chapter 6 constitutes the comparative case study, the most extensive chapter. Chapter 7 consolidates general conclusions and future research directions.

Chapter 2. HISTORICAL EFFECTS OF SEISMIC ACTION ON BRIDGES AND THE NEED FOR SEISMIC ISOLATION SYSTEMS

2.1 Lessons from major earthquakes

The study of major seismic events over recent decades has highlighted the extreme vulnerability of bridge infrastructure and has been the main driver for the evolution of standards and seismic protection technologies.

The Loma Prieta earthquake, California (1989, Mw = 6.9), caused the collapse of over 1300 m of the upper deck of the Cypress Street in Oakland, due to brittle shear failure of the columns resulting from insufficient transverse reinforcement and lack of confinement (Figure 1) [4, 5].

Figure 1. The collapse of the Cypress Street Viaduct during the Loma Prieta Earthquake [4, 5]

The Northridge earthquake, California (1994, $M_w = 6.7$), produced peak accelerations exceeding 1g in the epicentral area and severely damaged the Los Angeles Highway infrastructure. Main collapse causes included shear column failure, loss of deck bearing, and bending collapse, all characteristic of older, unretrofitted structures. Notably, all major damages occurred in structures not included in retrofit programs initiated after Loma Prieta [4, 6, 7].

The Kobe earthquake, Japan (1995, Mw = 6.9), caused severe damage over more than 20 km of the Hanshin Highway, with the collapse of massive reinforced concrete piers. Post-earthquake investigations showed that, despite design seismic forces being twice than those considered in the USA, reinforcement details favored brittle rather than ductile behavior. Importantly, the Hanshin Highway had not been included in restoration programs, since the Kobe area was considered to have low seismic hazard [4, 8].

Figure 2. The collapse of the Fukae Viaduct on the Hanshin Highway [9, 10]

The earthquake in Chile on 27 February 2010, with moment magnitude M_w 8.8, had its hypocenter at approximately 35 km depth and an epicenter about 8 km off the central Chilean coast. The seismic motion lasted at least 100 seconds, peak ground accelerations exceeded 0.60g both horizontally and vertically, causing over 830 damage incidents to road infrastructure [4, 6, 11].

2.2 Seismically isolated bridges – representative examples

The major seismic events described above have repeatedly demonstrated that the traditional design philosophy based solely on strength and stiffness is insufficient for adequate structural behavior under severe seismic loading.

In the United States, the Sierra Point Overhead was retrofitted in 1980 by replacing metal bearings with LRB isolators, and suffered no damage in the 1989 Loma Prieta earthquake.

In Italy, the San Giorgio Bridge in Genoa (2020), built to replace the collapsed Morandi Viaduct, is isolated by 51 Curved Surface Slider (CSS) devices. The Filomena Delli Castelli Bridge uses LRB isolators with equivalent damping exceeding 25%. The Somplago Viaduct, Europe's first seismically isolated bridge (1975–1980), withstood the 1976 Friuli earthquake without degradation [12].

In Romania, the Basarab Overpass (Figure 3) in Bucharest is the first bridge with a seismic protection system [4, 6], using LRB isolators and hydraulic dampers. On the A2 motorway, the bridge over the Danube–Black Sea Canal is equipped with Friction Pendulum System (FPS) isolators, while bridges on the Constanța bypass use HDRB isolators.

Figure 3. Basarab Overpass – the cable stayed bridge over the railway

Chapter 3. DESCRIPTION OF SEISMIC ACTION IN NATIONAL AND INTERNATIONAL STANDARDS

Romanian seismic regulations have evolved progressively, with each generation of standards reflecting advances in earthquake engineering knowledge and lessons from major seismic events of the past. The first mandatory national standard (P13-63) introduced the elastic spectrum with Tc = 0.30s. The 4 March 1977 Vrancea earthquake (Mw = 7.40) was a major turning point, demonstrating that the regulations then in force (P13-70) drastically underestimated real seismic forces. Standard P100-78, developed on the basis of the 1977 INCERC recordings, introduced the first structural ductility rules [13].

P100-2006 was the first partial alignment with Eurocode 8 and increased the mean recurrence interval from 50 to 100 years. P100-2013, currently in force, achieves full alignment with SR EN 1998-1, raising the MRI to 225 years (20% probability of exceedance in 50 years) and increasing the design ground acceleration for Bucharest to a_g = 0.30g (versus 0.24g in P100-2006). The structures analysed in this thesis are located in a zone with a_g = 0.20g (per P100-2006) and T_c = 0.70s.

Figure 4 presents a comparison between the normalized spectra β(T) and the absolute elastic response spectra S_e(T) for P100-1992, P100-2006 and P100-2013, along with the spectrum recorded in Bucharest during the March 4, 1977, Vrancea Earthquake.

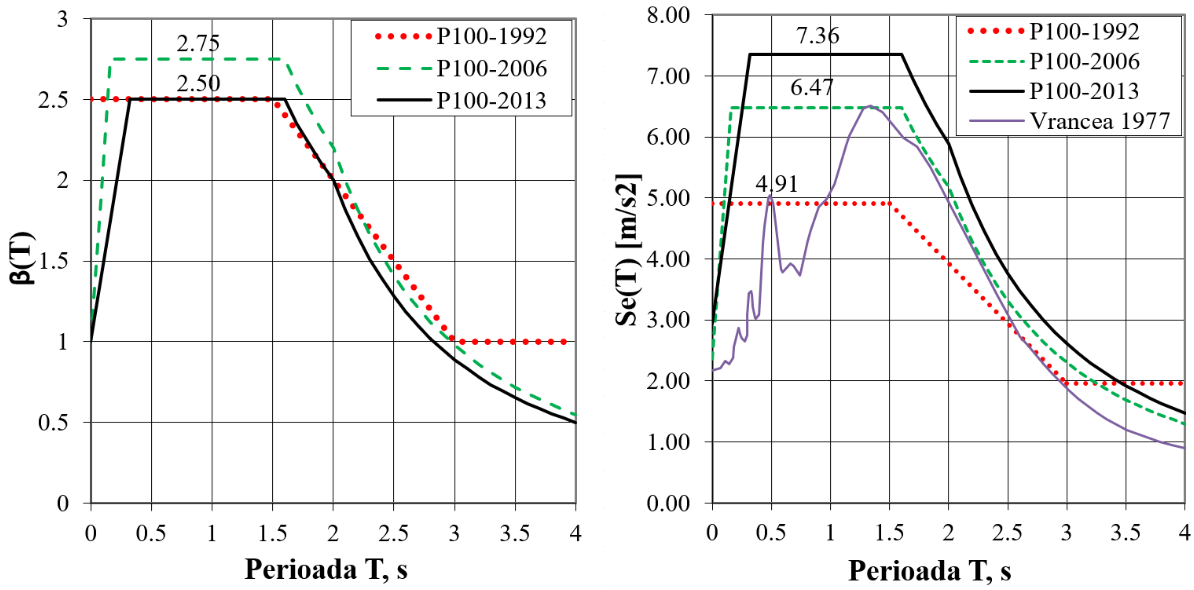

Figure 4. Comparison between normalized spectra (left) and response spectra (Bucharest, right) for the three design codes [14]

Chapter 4. TYPES OF SEISMIC ISOLATION DEVICES

Bridges located in areas where severe earthquakes may occur, and which have fundamental vibration periods in the range of high acceleration response, are subjected to significant inertial forces. This behavior often leads to structural deterioration involving both direct repair costs and indirect losses such as service disruption, traffic diversion, or even casualties. Traditional seismic analysis and design methods do not allow precise estimation of deformations and damage, making risk and loss assessment difficult [15].

The effective period of the isolation system is determined by (4-1):

$$T_{eff} = 2\pi\sqrt{\frac{W}{k_{eff}g}} \tag{4-1}$$

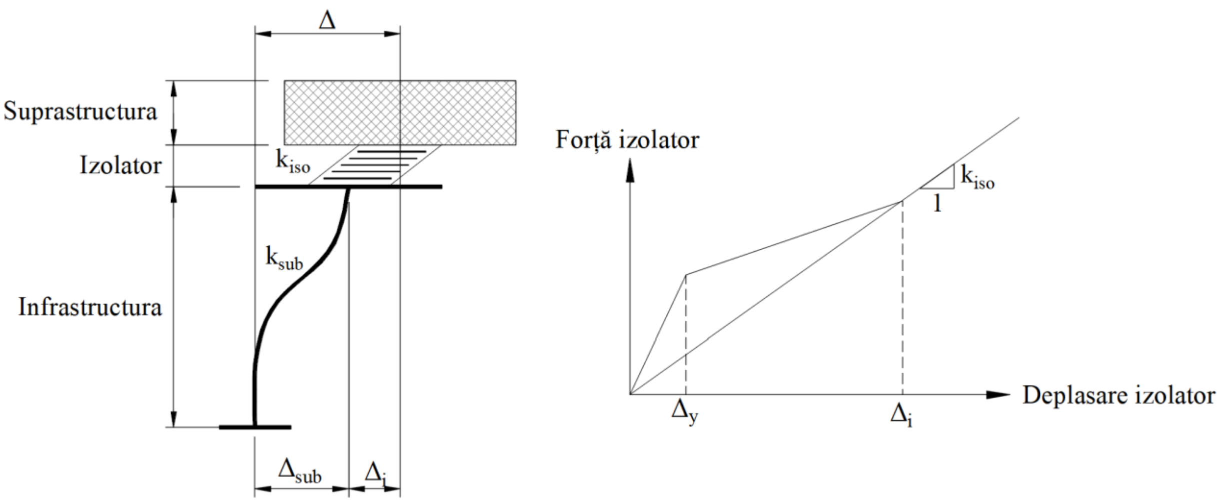

Figure 5. Effective lateral stiffness of the combined infrastructure-isolator system [16]

When calculating the effective stiffness k_{eff} (4-2), both the stiffness of the isolation devices and that of the substructure on which the isolators are placed must be taken into account(Figure 5):

$$k_{eff} = \frac{k_{sub} k_{iso}}{k_{sub} + k_{iso}} \tag{4-2}$$

4.1 High Damping Rubber Bearings (HDRB)

HDRB devices were developed in 1982 by the Malaysian Natural Rubber Producers Research Association, by adding extra-fine carbon, oils, and resins to natural rubber. The damping thus obtained reaches 10-20% at 100% shear deformation, depending on material hardness.

The material exhibits nonlinear behavior at low deformations (below 20%), characterized by high stiffness and damping, providing excellent performance under wind loading or low-intensity earthquakes. For shear deformations between 20-120%, the elastic modulus decreases and becomes nearly constant.

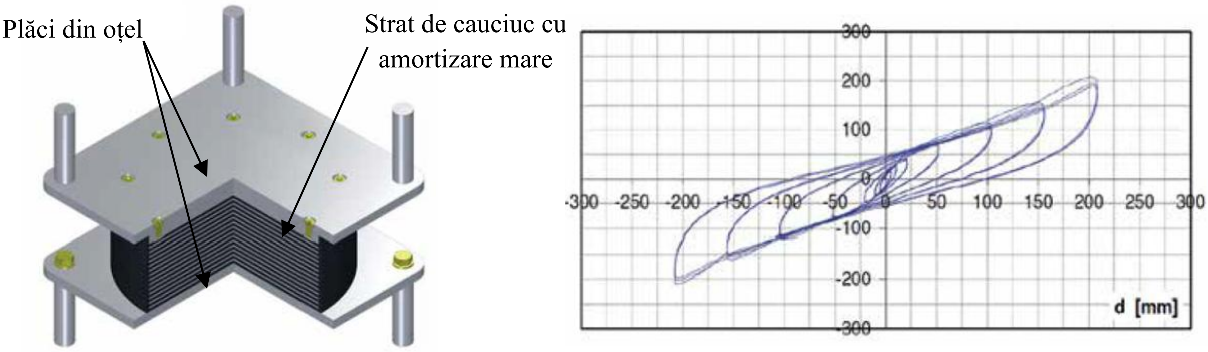

Figure 6. HDRB seismic isolator (left) and its hysteretic curve (right) [4, 17]

4.2 Lead Rubber Bearings (LRB)

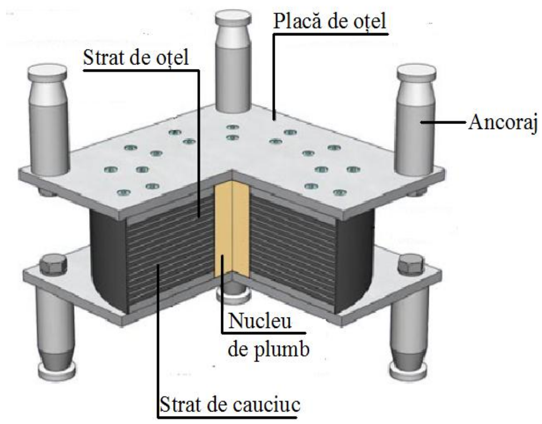

Figure 7. LRB Seismic isolator [18]

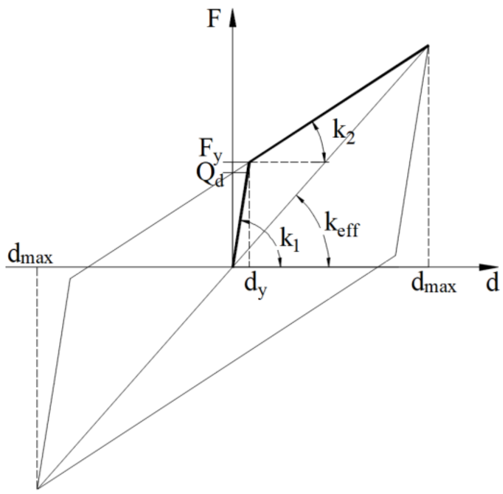

Figure 8. LRB bilinear model parameters [19, 20]

These devices consist of thin steel plates to which rubber strips are vulcanized. Additionally, the device contains lead bars inserted into cavities. The behavior of LRB is hysteretic but can be approximated as bilinear, considering an elastic and a post-yield stiffness. Once the lead yield limit is reached, the lateral stiffness of the device is provided solely by the elastomeric layers [20, 21, 22]. The bilinear behavior is characterized by three parameters: k_1, k_2, and Q (Figure 8).

4.3 Friction Pendulum System (FPS)

It consists of an articulated piece that slides by friction on a smooth concave surface coated with a low-friction-coefficient material. A major advantage is its capacity to return to the initial position, preventing large residual deformations after an earthquake that could compromise structural functionality and the maximum displacement capacity of the bearing device [23, 24, 25].

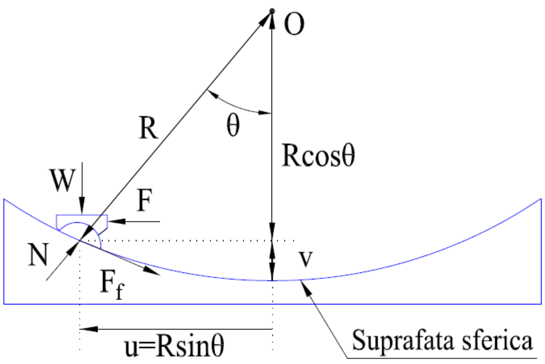

Figure 9. Force equilibrum on the sliding surface [6, 26]

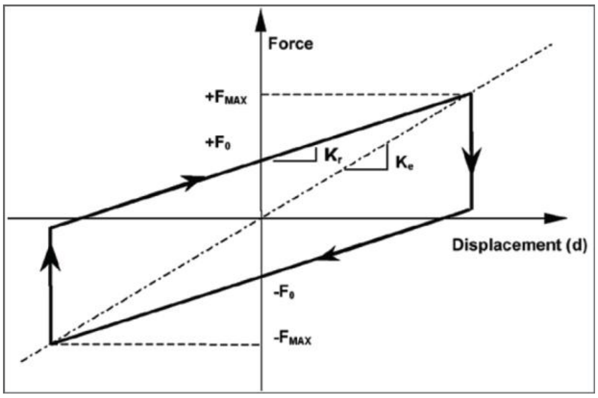

Figure 10. Idealized bilinear curve [27, 28]

The most important parameter of this device is the vibration period T. Considering the vertical load on the isolator N_{Sd}, the horizontal displacement d, and the friction coefficient μ, the maximum horizontal force F_{max} is defined as (4-3):

$$F_{max} = F_0 + K_r \cdot d = \mu \cdot N_{Sd} + \frac{N_{Sd}}{R} \cdot d \tag{4-3}$$

Chapter 5. METHODOLOGIES FOR ASSESSING BRIDGE VULNERABILITY TO SEISMIC ACTION

5.1 Behavior factor, q

The behavior factor is defined globally for the entire structure and reflects its ductility, understood as the structure's capacity to withstand, with acceptable deterioration but without failure, seismic actions in the post-elastic range. The behavior factor q characterizes the type of structural behavior, which can be dissipative or non-dissipative.

Figure 11 illustrates a typical relationship between base shear and roof displacement of a structure, which is idealized by a bilinear relationship [29].

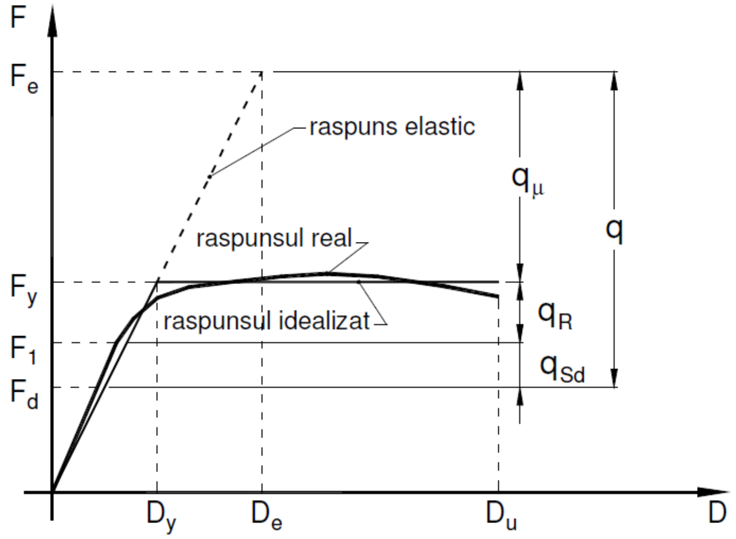

Figure 11. Components of the behavior factor, q [29, 30, 31]

The final value of the behavior factor is defined as the product of the three previously mentioned coefficients [29, 30]:

$$q = q_{\mu} \cdot q_{Sd} \cdot q_R \tag{5-1}$$

5.2 Seismic performance assessment using nonlinear static analysis (Pushover)

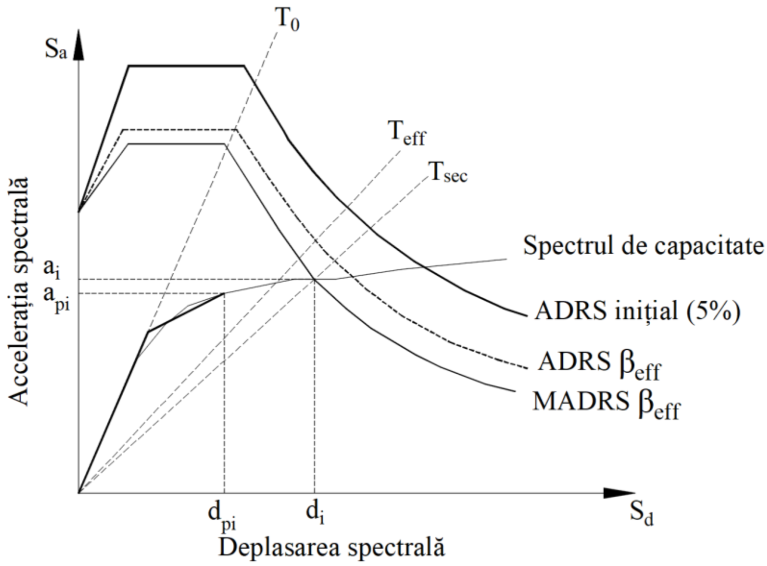

Figure 12. Performance point determination using Procedure B from FEMA440 [2]

Pushover analysis determines the capacity curve (base shear force vs. top displacement) by applying monotonically increasing lateral forces. On this curve, the sequence of plastic hinge formation and failure mechanisms is identified. The performance point (intersection of capacity spectrum and demand spectrum) is determined using the MADRS equivalent linearization procedure from FEMA 440 (Method B, Figure 12). This methodology is superior to the classic ATC-40 method, offering a more accurate estimate of effective period and effective damping, validated through comparative studies on perfect elasto-plastic oscillators.

5.3 Incremental Dynamic Analysis (IDA)

The IDA method, introduced by Vamvatsikos and Cornell (2002) [32], involves subjecting the structural model to a set of ground motion records progressively scaled to successive intensity levels. For each intensity level, a nonlinear Time-History dynamic analysis is performed by direct integration, obtaining IDA curves describing the evolution of a damage parameter (plastic hinge rotation, for example) as a function of seismic intensity (scaling factor Fs).

Fragility curves are constructed using lognormal statistical modeling of IDA results for each intensity level, expressing the non-exceedance probability of a considered performance threshold. The total dispersion of the damage parameter characterizes uncertainties associated with the variability of seismic records.

Chapter 6. COMPARATIVE STUDY: SEISMIC RESPONSE OF FOUR PRESTRESSED CONCRETE CONTINUOUS-GIRDER BRIDGES

6.1 Description of the Analysed Structures

Four prestressed concrete continuous-girder bridges (S2-S5), with 2 to 5 spans of 40 m, were analysed. All structures share the same superstructure characteristics: prefabricated prestressed girders H = 2.10m (C50/60 concrete), minimum 20cm in-situ slab (C35/45 concrete), and a 12.00m carriageway. The substructure consists of two-column circular piers D = 2.00 m (C30/37 concrete), founded on bored piles ϕ1.20 m (Figure 13)..

The main variables are the number of spans and pier heights: S2 (2 spans, Pier P1 = 8.00m), S3 (3 spans, P1 = 8.00m, P2 = 10.00m), S4 (4 spans, P1 = 7.00m, P2 = 11.00m, P3 = 9.00m), S5 (5 spans, P1 = 8.00m, P2 = 11.00m, P3 = 9.00m, P4 = 6.00m). Non-uniform pier heights generate unequal lateral stiffness distributions, with direct consequences on behavior factor values.

The design seismic action was defined as per P100-1/2006, with a_g = 0.20g and Tc = 0.70s. For initial design, the design spectrum with q = 1.50 was used. The 16 structural models (4 bridges x 4 bearing systems) were coded as SX-Y, where X = number of spans and Y = bearing type (N, P, LRB, FPS).

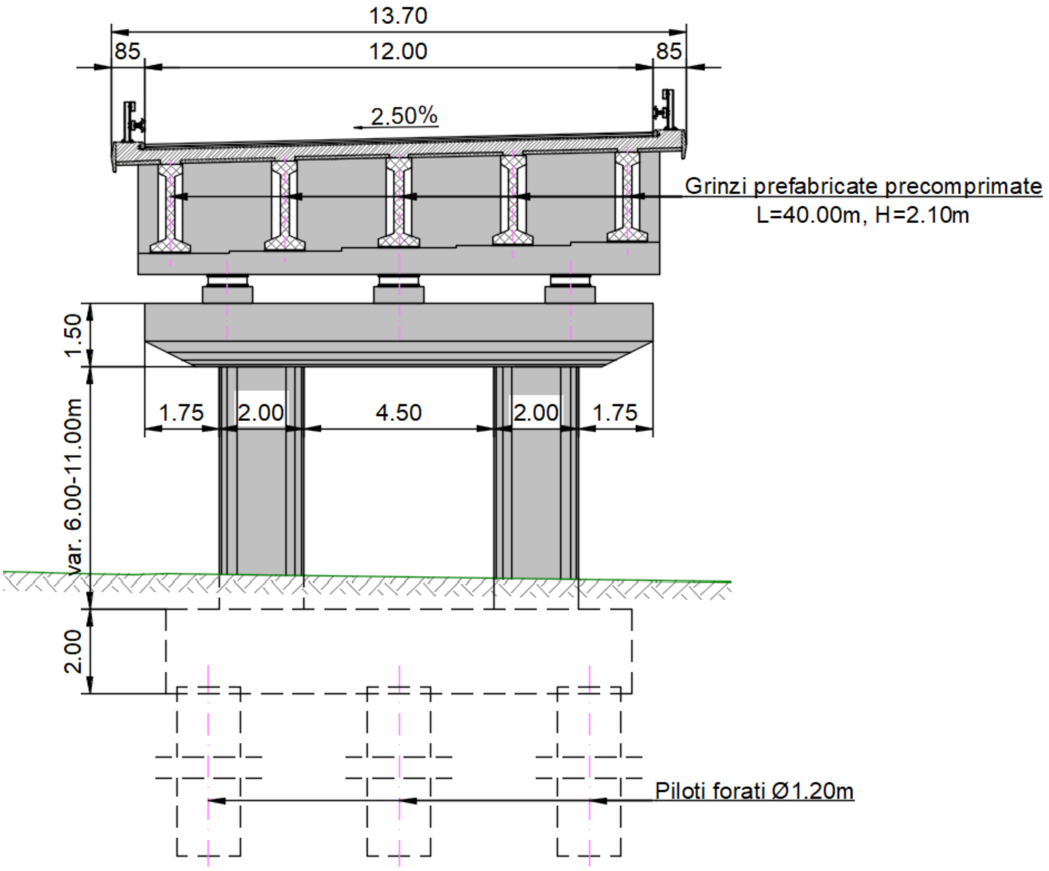

Figure 13. Cross section of the analized bridges

6.2 Finite element model parameters

Finite element models were developed in CsiBridge [33]. Prefabricated girders were modeled with frame elements, the in-situ slab with shell elements, and the connection between them with rigid links. Pier columns and bored piles were modeled with frame elements, and pile-soil interaction with springs placed at 1m intervals. Bearings were introduced as links with mechanical properties corresponding to each type. Stiffness parameters for movable neoprene bearings: H_{max} = 500kN, Δ_{max} = 10.00 cm, k_h = 5000 kN/m.

LRB isolators were designed for a target fundamental period T_1 = 2.50 s: characteristic resistance Q_d = 99.00kN (abutments) / 264.00kN (piers), effective stiffness k_{eff} = 1127kN/m (abutments) / 2920.00kN/m (piers), design displacement d_{bd} = 210mm and maximum displacement d_{Ed} = 350 mm. FPS isolators have a radius of curvature R = 3100mm, friction coefficient μ_{fast} = 0.08, and maximum displacement d_{Ed} = 300 mm, yielding fundamental periods of 2.84–2.87s.

6.3 Linear Dynamic Analysis – Initial Design

Modal spectral analysis provided the fundamental periods and forces needed for pier reinforcement design, kept constant across all bearing configurations. Fundamental periods range from 0.75s (S2) to 1.05s (S5), with participating masses of 91–93% in vibration mode 1.

Maximum bearing displacements remained within the admissible limits of the elastomeric bearings used (below 10cm), validating the design for the design earthquake.

6.4 Seismic performance assessment using Pushover Analysis

6.4.1 Performance point and behavior factor determination for the reference support system (neoprene bearings)

Pushover analysis revealed that neoprene bearings significantly limit the seismic capacity of the analyzed bridges. For structures S3, S4, and S5, the seismic displacement demand exceeds the nominal capacity of the movable bearings (Δ_{max} = 10cm) already at MRI = 225 years, activating anti-seismic stoppers and changing the static scheme. The total behavior factor ranges from q = 1.63 (S2, MRI = 100 years) to q = 3.57 (S3 and S4, MRI = 2475 years). High q values at extreme levels do not reflect superior performance, but increasingly large excursions into the post-elastic range, with significant uncertainties regarding bearing system integrity.

Figure 14 shows that structural redundancy increases with the number of spans (q_R = 1.17 for S2-N compared to 1.60 for S5-N at MRI = 2475 years), while ductility decreases (q_μ = 2.89 for S2-N compared to 2.12 for S5-N at the same hazard level). Structure S2-N, characterized by a simple plastic mechanism (a single pier with a fixed bearing), is the only one that maintains displacements below the allowable limit up to MRI = 475 years.

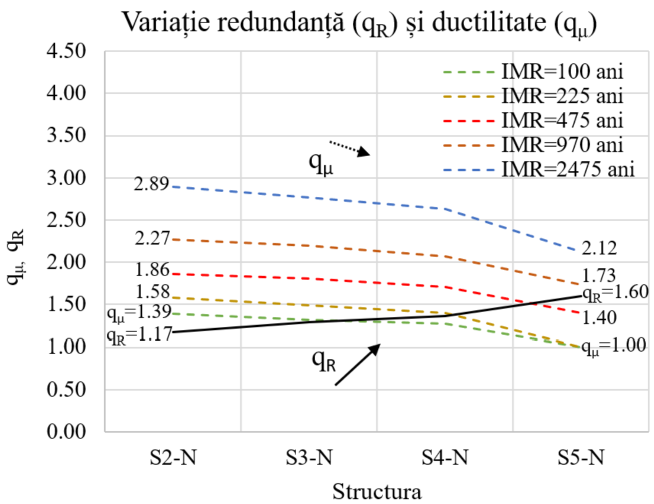

Figure 14. Evolution of structural redundancy and ductility with the number of spans

6.4.1 Performance point and behavior factor determination for the pot bearings system

The transition from neoprene bearings to pot bearings evaluated structural response under the larger displacements permitted by pot bearings.

Their use reduces spectral accelerations by 28-54% compared to neoprene eqquiped structures, by decreasing global stiffness and increasing effective periods. Maximum reduction of 54% was recorded at S5 for MRI = 475 years, minimum of 28% at S4 for MRI = 2475 years. Behavior factors are higher than for neoprene (q = 1.73-1.86 at MRI = 100 years vs. 1.23–1.73), indicating larger post-elastic deformations.

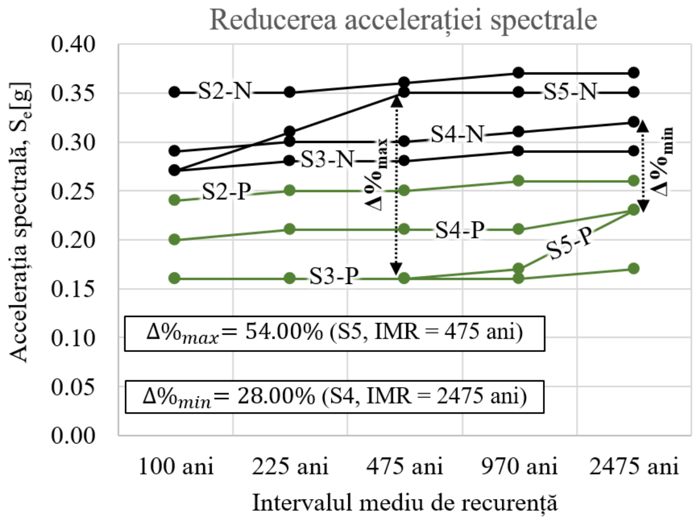

Figure 15. Comparison of spectral acceleration values for structures with neoprene and pot bearings

Although pot bearings show degradation only for structures S3-P and S5-P at MRI = 2475 years, behavior factor values indicate significant structural post-elastic deformations under severe seismic action. High q values reflect energy dissipation based on significant structural degradation at pier level through plastic hinge formation.

6.4.1 Performance point and behavior factor determination for support system with LRB (Lead Rubber Bearings)

Introduction of LRB isolators fundamentally changes structural behavior. The effective behavior factor is q = 1.00 for all structures and all hazard levels, meaning piers remain in the elastic range. The effective damping provided by the isolators is β_{eff} = 25-31%. Spectral acceleration reductions compared to neoprene bearings are 40-74% (minimum 40% at MRI = 2475 years and S5, maximum 74% at MRI = 100 years and S2). Compared to pot bearings, reductions range between 6% and 62.5%.

6.4.1 Performance point and behavior factor determination for support system with FPS (Friction Pendulum System)

The FPS system offers the best overall seismic performance. Secant periods of 2.11-2.73s (higher than LRB periods of 1.93-2.32s) lead to the smallest spectral accelerations of all configurations analysed (below 0.10g at MRI = 100 years vs. over 0.35g for neoprene). Effective damping is β_{eff} = 26-33%. The behavior factor is q = 1.00 for all cases (Figure 16).

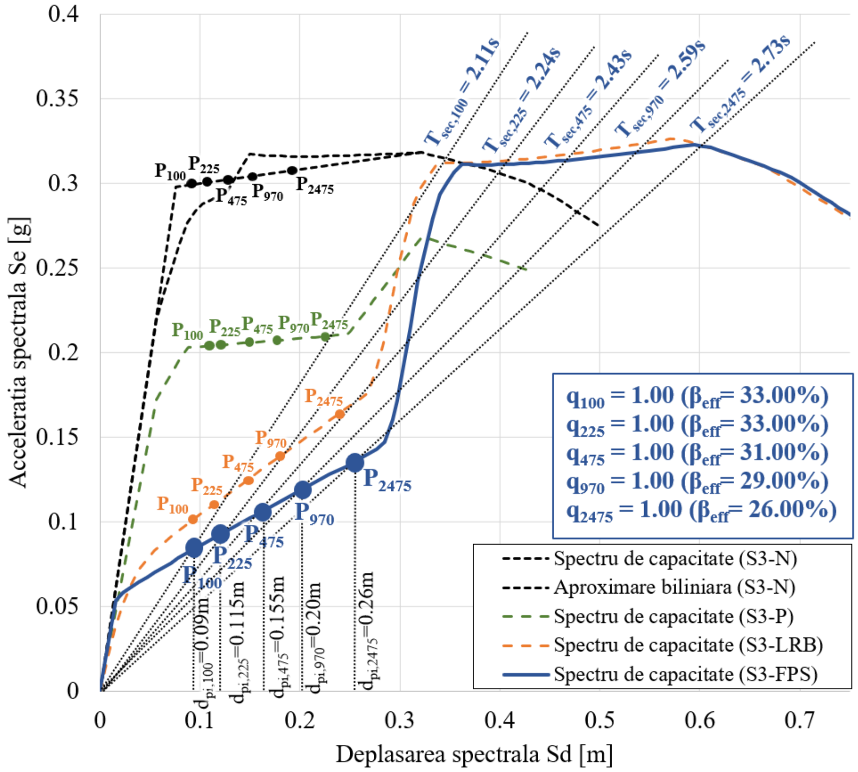

Figure 16. Performance points and behavior factors obtained (S4-FPS bridge); Comparison with previously obtained performance points

Figure 17 shows a significant decrease in spectral accelerations S_e for the isolated structures compared to the non-isolated ones, confirming their high efficiency.

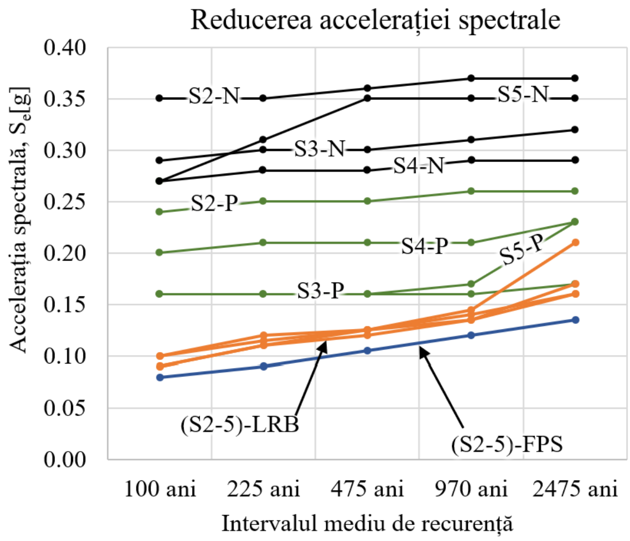

Figure 17. Comparison of spectral acceleration values for all analyzed configurations

According to Figure 18, the largest reductions in spectral accelerations were recorded for earthquakes with more frequent return periods (MRI = 100 years and 225 years, respectively). In the case of structures equipped with pot bearings, the spectral acceleration values range between approximately 50% and 70% of the reference system values, while for the isolated systems (LRB and FPS), the reductions are significant, with proportions ranging between 23% and 37%.

On the other hand, Figure 19 presents the highest ratios relative to the reference (the smallest reductions), which occur under the extreme scenario (MRI = 2475 years); these range between 59% and 72% for configurations with pot bearings, and 36%-60% for isolated systems, respectively.

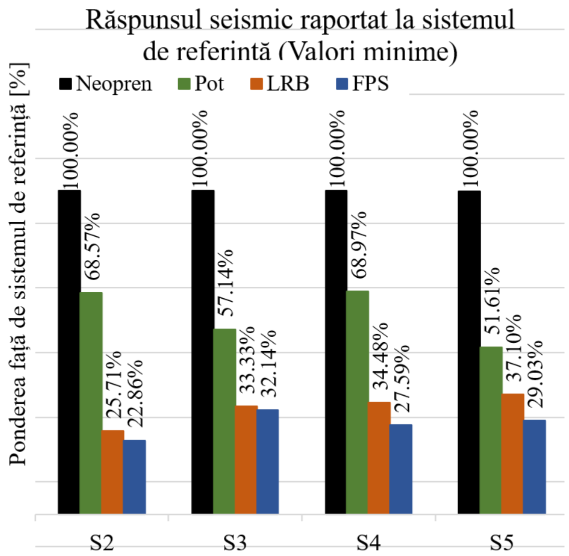

Figure 18 Minimum spectral acceleration ratios of Pot, LRB, and FPS systems relative to the Neoprene reference system (MRI = 100, 225 years)

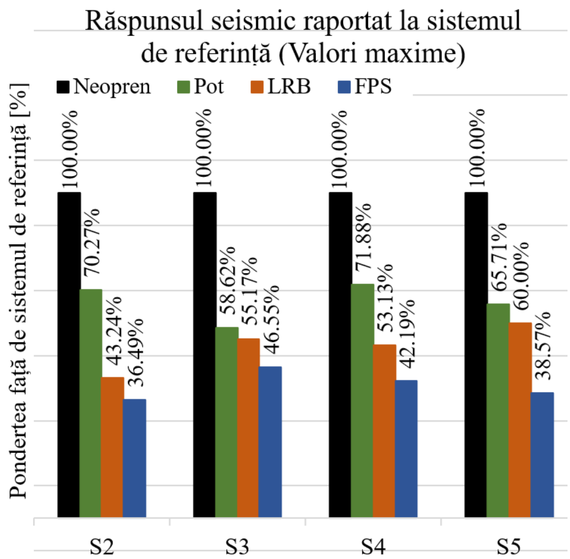

Figure 19. Maximum spectral acceleration ratios of Pot, LRB, and FPS systems relative to the Neoprene reference system (MRI = 100, 225 years)

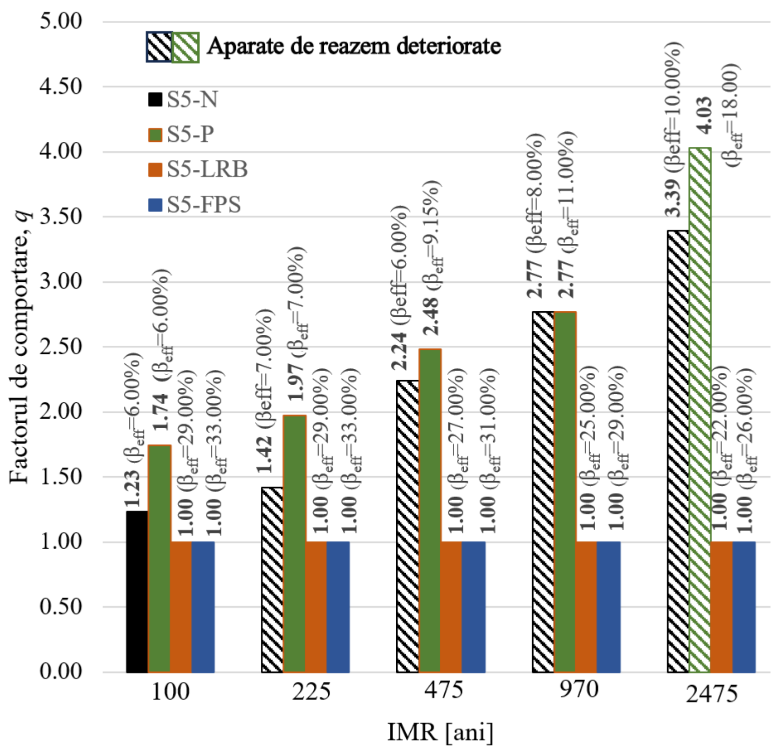

Figure 20. Comparative analysis of behavior factors (q) and effective damping (β_{eff}), for S5

The efficiency of the isolation systems is also demonstrated by the correlation between the behavior factor q and the effective damping β_{eff}, presented in Figure 20 for structure S5.

The results obtained using nonlinear static Pushover analysis and the equivalent linearization process (the MADRS method according to FEMA 440) highlighted the superiority of isolation systems by maintaining the structural response within the elastic range and providing high damping without pier degradation. However, the static nature of this method has limitations in capturing complex dynamic effects and the variability of real seismic records.

To validate these observations, the next chapter examines the dynamic response of the structures under a set of scaled artificial accelerograms, using Incremental Dynamic Analysis (IDA).

6.5 Vulnerability assessment through Incremental Dynamic Analysis (IDA)

6.5.1 Generation of artificial accelerograms

Seven artificial accelerograms (Figure 21) compatible with the elastic response spectrum at the site (MRI = 100 years) were generated using SeismoArtif v2026 [34]. Each accelerogram has a duration of 20 seconds. The mean spectrum of the 7 accelerograms falls within the normative limits (±10% of the reference elastic spectrum) [29, 35]. Scaling for other hazard levels was performed using scaling factors $Fs = (T_{Rc}/T_{NRC})^k$, with k = 0.3 per SR EN 1998-1. Total analyses: 4 structures x 4 bearing systems x 7 accelerograms x 5 MRI levels = 560 nonlinear Time-History direct integration analyses.

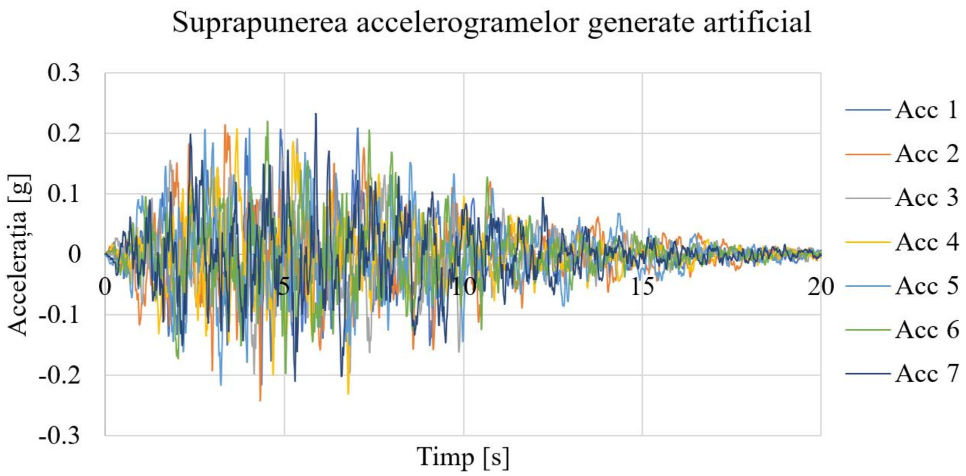

Figure 21. Superposition of the 7 artificially generated accelerograms

6.5.2 Comparative study of Time-History Analysis Results

The most important finding from the dynamic analyses is that for structures equipped with LRB or FPS isolators, no plastic hinge rotations were recorded at piers in any of the 560 Time-History analyses performed. Seismic energy is dissipated exclusively at the level of isolation devices. Force-displacement diagrams of the isolators show nearly identical behavior for all four structures (S2-S5) under the same seismic input, demonstrating that seismic response is governed primarily by device properties rather than infrastructure geometry (figurile 22-25)..

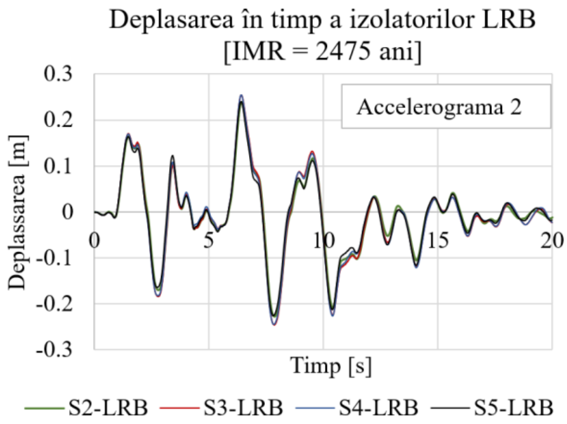

Figure 22. Superposition of displacement time-history for LRB isolators (results for MRI = 2475 years, Accelerogram 2)

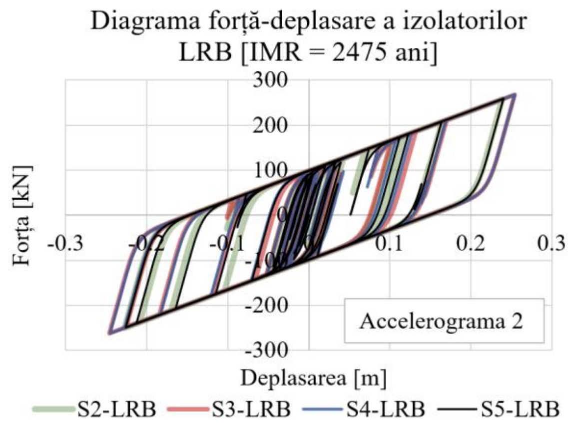

Figure 23. Superposition of force-displacement diagrams for LRB isolators (results for MRI = 2475 years, Accelerogram 2)

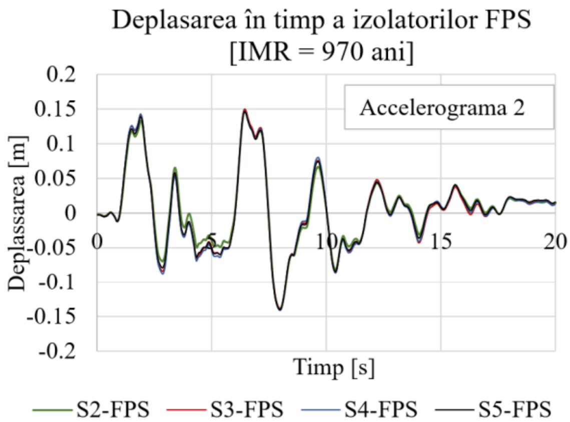

Figure 24. Superposition of displacement time-history for FPS isolators (results for MRI = 970 years, Accelerogram 2)

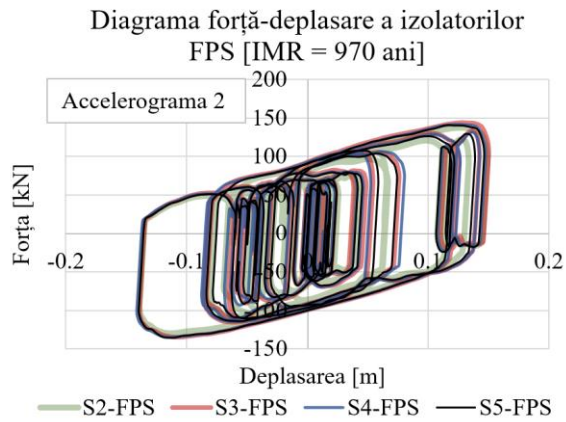

Figure 25. Superposition of force-displacement diagrams for FPS isolators (results for MRI = 970 years, Accelerogram 2)

Reductions in bending moments at pier bases compared to neoprene bearings are 45–75% for LRB isolators (maximum 75% at S2 and MRI = 100 years, minimum 45% at S3 and MRI = 2475 years) and 61-80% for FPS isolators (maximum 80% at S2 and MRI = 100 years, minimum 61% at S4 and MRI = 2475 years).

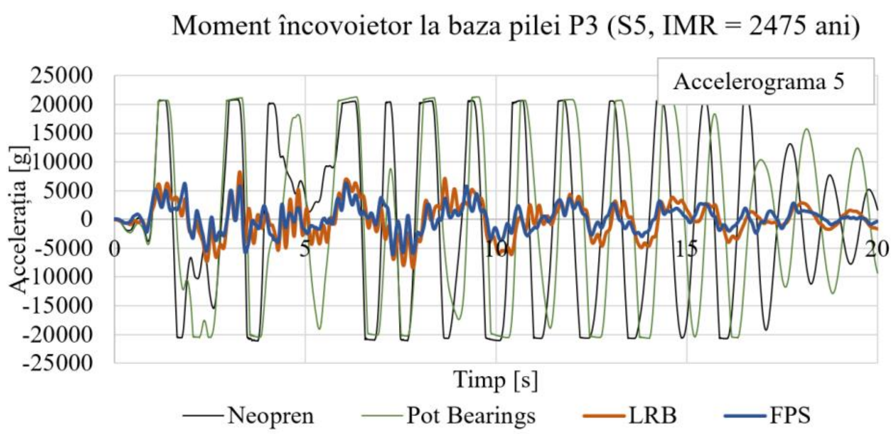

Figure 26. Bending moment time-history (Structure S5, MRI = 2475 years, Accelerogram 5)

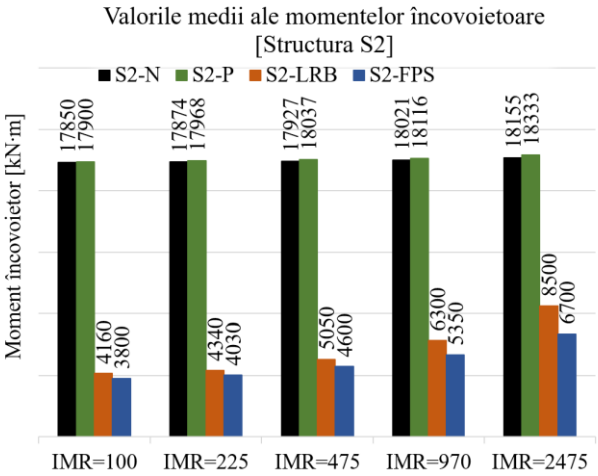

Figure 27. Mean values of maximum bending moments for the 7 accelerograms (Structure 2, Pier P1)

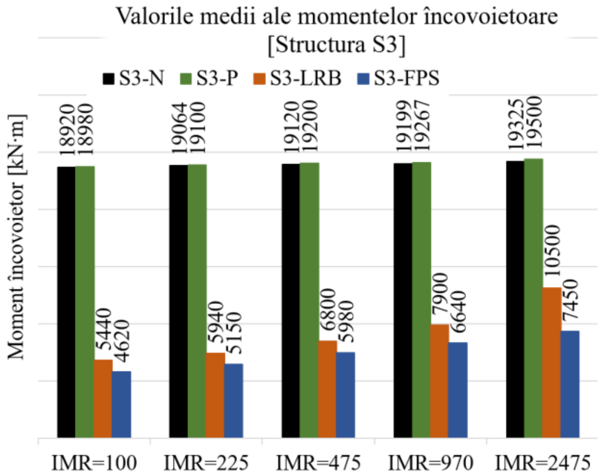

Figure 28. Mean values of maximum bending moments for the 7 accelerograms (Structure 3, Pier P1)

6.5.1 IDA curves and fragility curves

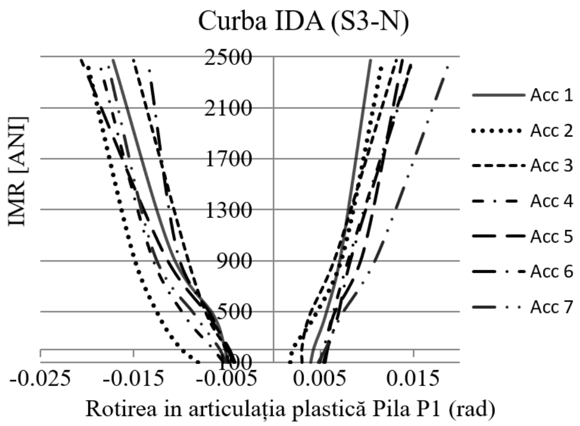

Figure 29. IDA curves for S3-N

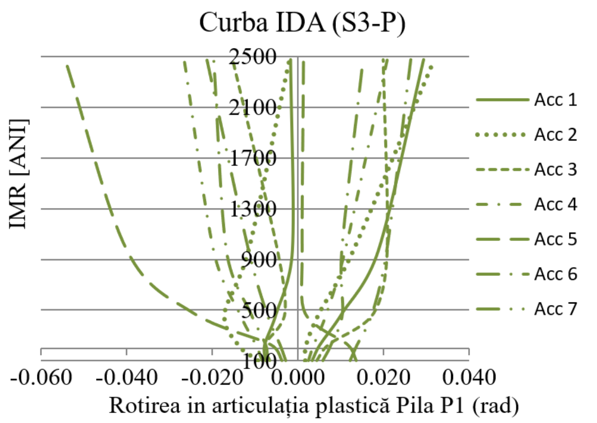

Figure 30. IDA curves for S3-P

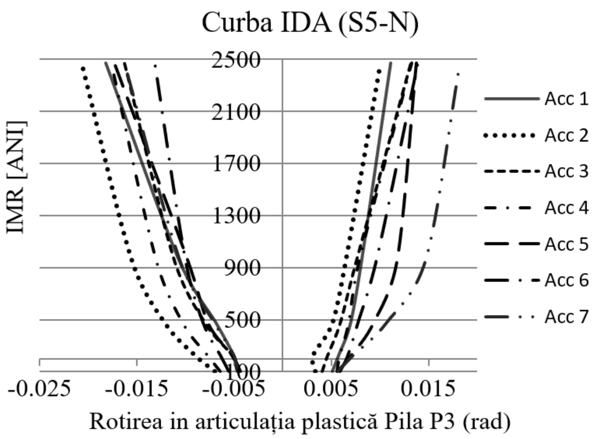

Figure 31. IDA curves for S5-N

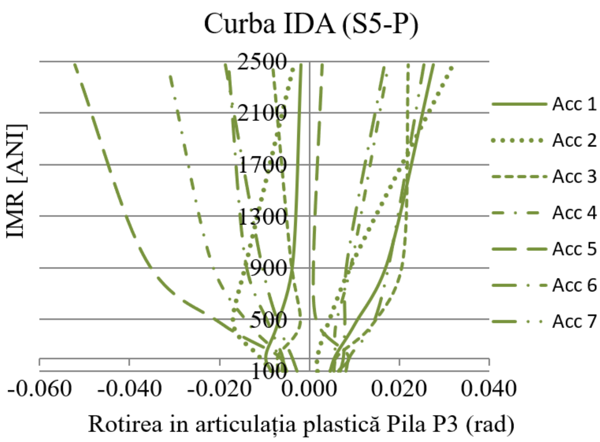

Figure 32. IDA curves for S5-P

IDA curves (figures 29-32) are presented for structures equipped with neoprene (N) and pot (P) bearings, for which plastic hinge rotations at pier bases were recorded at all seismic hazard levels analysed. For structures with LRB and FPS isolators, construction of IDA curves based on plastic hinge rotation is not possible, as piers remained elastic in all analyses. The absence of plastic deformations confirms that LRB and FPS seismic isolation systems fully achieve their fundamental objective: protecting the structure by dissipating seismic energy exclusively at the isolation device level.

The next stage consists of evaluating the structural behavior from a performance perspective using fragility curves. These represent cumulative distribution functions that express the probability that a structural response indicator (in this case, the plastic hinge rotation at the pier base) will exceed a given performance threshold, as a function of the seismic intensity [6]. Fragility curves (figures 33-34) were constructed for performance levels defined in FEMA 356 [3]: Immediate Occupancy (IO), Life Safety (LS), and Collapse Prevention (CP), with plastic hinge rotation thresholds:

Table 1. Performance levels for the plastic hinge rotation, θ (rad)

Parametru	IO	LS	CP
Rotire articulație plastică (θ)	0.003	0.012	0.015

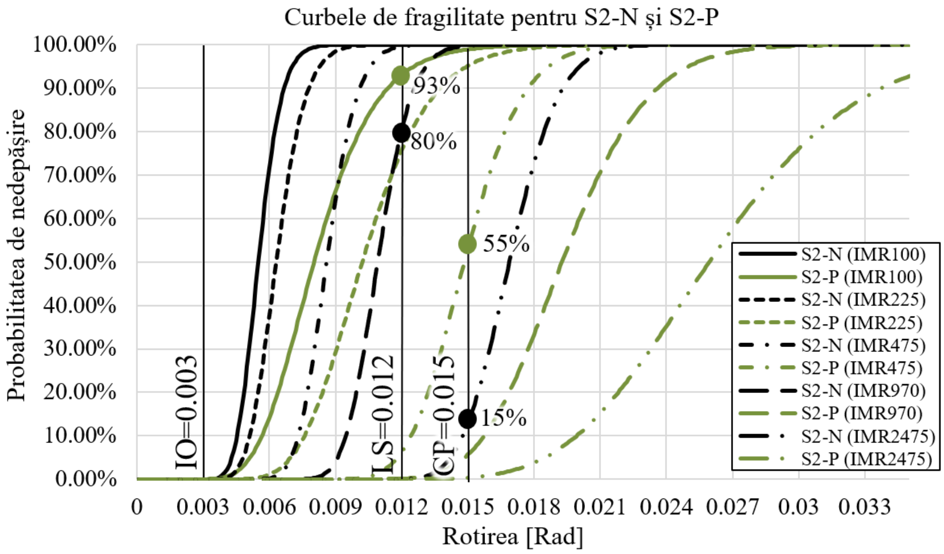

Figure 33. Fragility curves for S2-N and S2-P

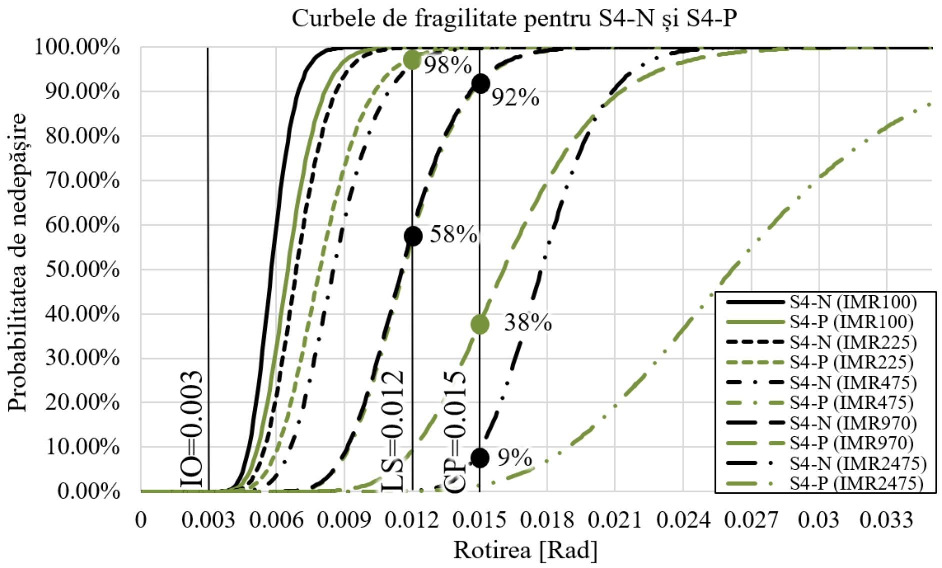

Figure 34. Fragility curves for S4-N and S4-P

Figure 35 presents comparative plots of the non-exceedance probabilities for each structure, for the CP performance level.

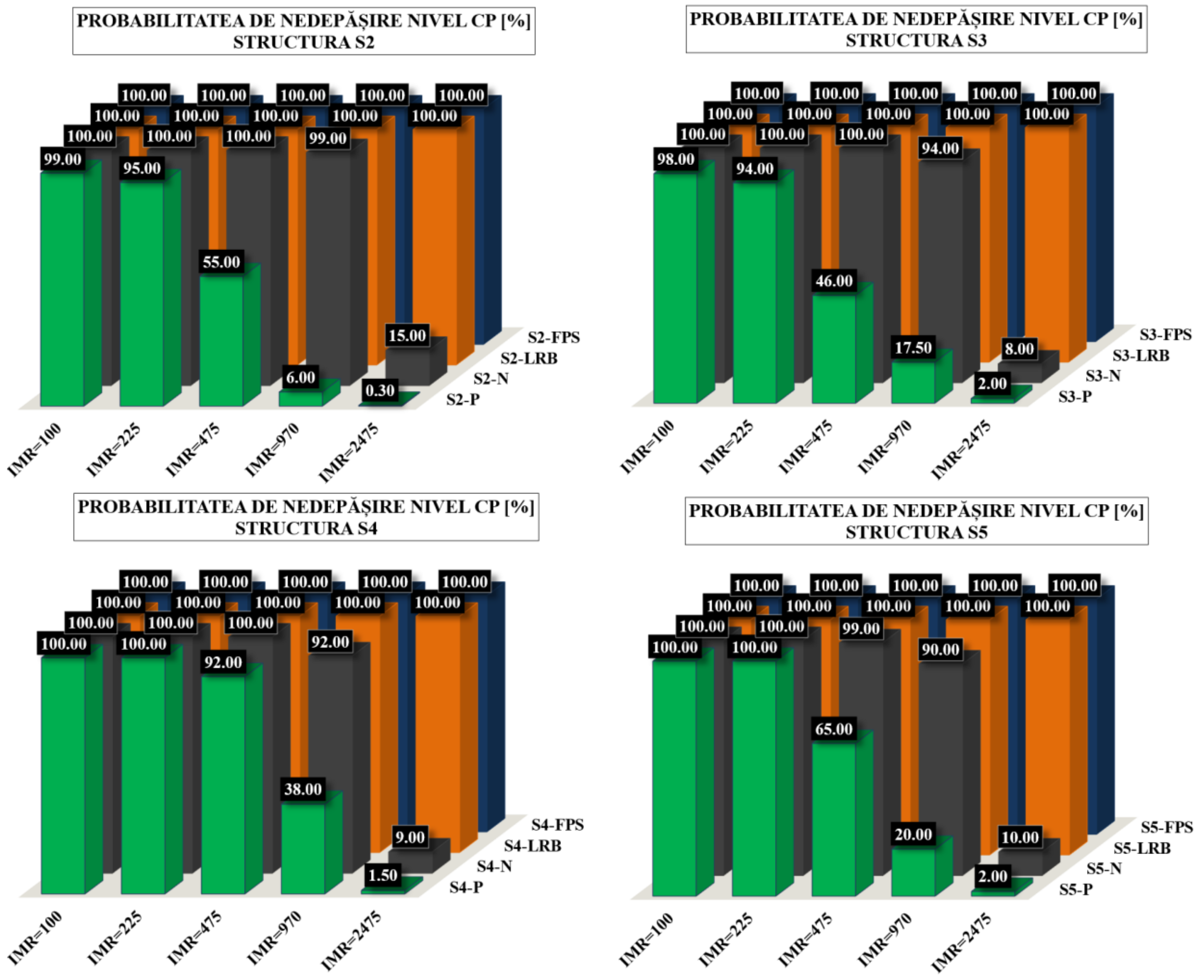

Figure 35. Non-exceedance probabilities for the CP performance level

Key findings from fragility curve analysis:

- *IO level (θ = 0.003 rad):* Non-exceedance probability is zero for all structures at all hazard levels, regardless of the non-isolated bearing system. Rotations exceed the IO threshold even at MRI = 100 years, consistent with behavior factor q > 1.00 from obtained from the Pushover analysis;

- *LS level (θ = 0.012 rad):* Non-exceedance probabilities are 100% at MRI = 100 and 225 years for neoprene, dropping to 93–99% at MRI = 475 years and 44-80% at MRI = 970 years. At MRI = 2475 years they become zero. Pot bearing structures degrade faster (LS probability of only 6.3% at MRI = 475 years for S2-P vs. 99% for S2-N);

- *CP level (θ = 0.015 rad):* Probabilities remain high (90-100%) up to MRI = 970 years for neoprene, but drop to 8-15% at MRI = 2475 years. For pot bearings, they drop to 0.3-2% at MRI = 2475 years. Isolated structures (LRB and FPS) record 100% non-exceedance probabilities for LS and CP at all hazard levels.

6.5.2 Correlation between behavior factor q and non-exceedance probability P%

An original applied result of this thesis is the lognormal statistical correlation between the behavior factor q, determined via Pushover analysis, and the non-exceedance probability P% of the LS and CP performance levels, determined via IDA. The analysis identified the critical interval q ∈ [2.50; 3.00], corresponding to MRI = 475-970 years, beyond which LS and CP non-exceedance probabilities rapidly decline toward zero.

The q-P% correlation allows bridge design engineers to rapidly estimate the seismic vulnerability of continuous-girder prestressed concrete bridges of similar typology, without requiring a full set of nonlinear dynamic IDA analyses. Neoprene structures exhibit higher non-exceedance probabilities than pot-bearing structures at the same q factor level, but this conclusion refers exclusively to infrastructure response, without considering bearing condition (neoprene bearings degrade faster).

Figure 36 presents the correlation between q and P\% as a function of the results specific to each bearing type (neoprene or pot bearing). It can be observed that the neoprene-supported structures exhibit higher non-exceedance probabilities compared to the structures with pot bearings, for both LS and CP performance levels.

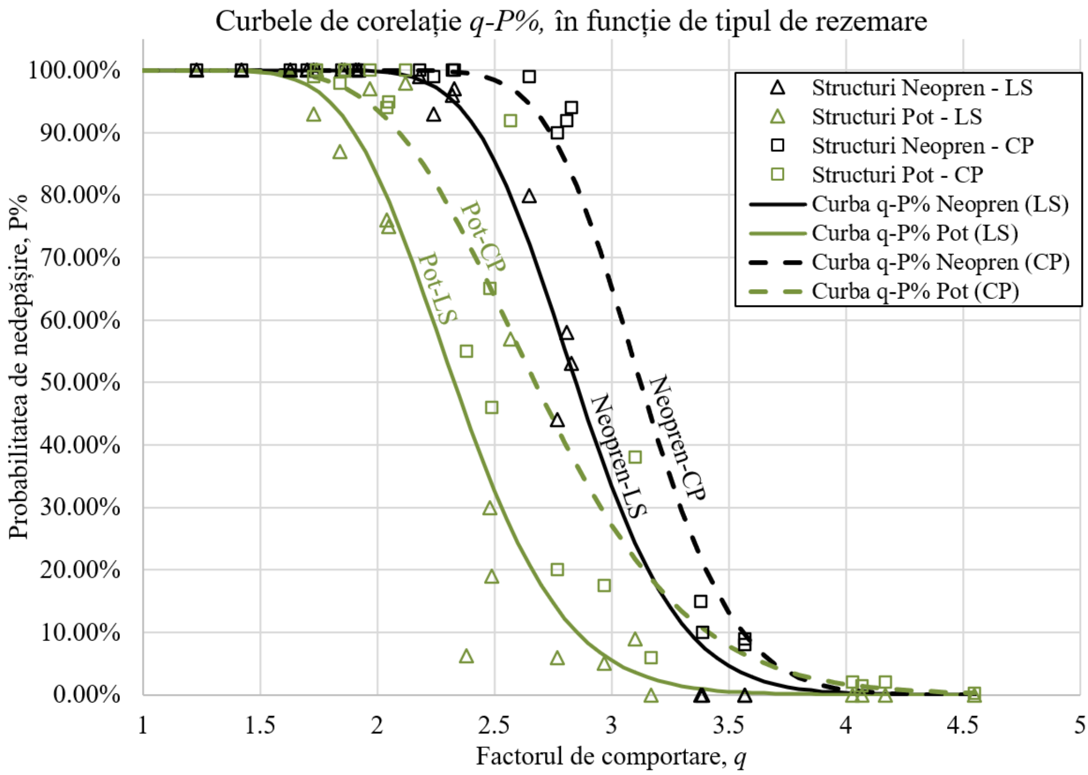

Figure 36. q-P% correlation, for neoprene and pot bearings systems

Chapter 7. GENERAL CONCLUSIONS

7.1 Conclusions on conventional bearing systems

Neoprene elastomeric bearings, while ensuring seismic performance at the design earthquake (MRI = 100 years, LS non-exceedance probability = 100%), exhibit significant vulnerability at higher hazard levels. Premature degradation of movable bearings, which exceed the nominal displacement capacity (Δ_{max} = 10cm) already at MRI = 225 years for structures S3–S5, followed by activation of anti-seismic stoppers and modification of the static scheme, represents the predominant vulnerability mechanism for the analysed typology.

Pot bearings reduce spectral accelerations by 28–54%, but do not substantially improve structural behavior of piers compared to neoprene. Their nearly zero stiffness of the movable bearings leads to reduced global stiffness, allowing larger pier post-elastic deformations. Their main advantage lies in maintaining bearing integrity at higher hazard levels compared to neoprene.

7.2 Conclusions on seismic isolation systems (LRB și FPS)

Results obtained via both methodologies (Pushover and IDA) clearly confirm the superiority of seismic isolation systems. The effective behavior factor is q = 1.00 for all configurations and all hazard levels analysed; piers remain in the elastic range with 100% non-exceedance probability for LS and CP across all 560 nonlinear dynamic analyses. Seismic energy is dissipated exclusively at device level.

The FPS system proves superior to LRB through: higher secant periods (2.11-2.73 s vs. 1.93-2.32 s), higher damping (β_{eff} = 26-33% vs. 25-31%), lower spectral accelerations (below 0.10g vs. below 0.15g at MRI = 100 years), and greater bending moment reductions (61-80% vs. 45-75%). The essential advantage of FPS is automatic return to initial position under gravitational effect, preventing post-earthquake residual deformations.

LRB or FPS seismic isolation systems are recommended as a priority for bridges located in zones with ag ≥ 0.20g, especially for those with variable pier heights or complex configurations, where non-uniform stiffness distributions can amplify seismic vulnerability.

7.3 Conclusions on the q-P% correlation

The critical interval q ∈ [2.50; 3.00] identified in this study corresponds to the MRI = 475-970 year transition domain, beyond which LS and CP non-exceedance probabilities rapidly decline toward zero for the analysed typology.

7.4 Future research directions

Based on the obtained results, the following directions for future research are proposed:

1. Extension of the study to other bridge typologies (steel or composite girders, viaducts with tall piers, etc.);
2. Analysis of seismic action in the transverse direction and combination of bidirectional loading, particularly for curved or skewed bridges;
3. Study of soil-structure interaction effects on the response of isolated systems;
4. Experimental validation of the q–P% correlation on reduced-scale physical models.
5. Investigation of seismic behavior of isolated bridges in Vrancea-specific earthquake scenarios using natural accelerograms recorded in Romania, to evaluate the influence of the frequency content and duration specific to the Vrancea zone on isolators efficiency.

7.5 Dissemination of research results

The results of this thesis have been disseminated in the scientific community through the publication of two scientific articles directly related to the research topic. Aspects regarding methodologies for assessing bridge performance under seismic action were published in *"Methodologies for assessing bridge performance under seismic action*", Romanian Journal of Transport Infrastructure, vol. 15 (2026), no. 1, in collaboration with Prof. Dr. Eng. Răcănel Ionuț Radu and Assoc. Prof. Dr. Eng. Urdăreanu Vlad Daniel. Additionally, the seismic vulnerability assessment of reinforced concrete bridges via Incremental Dynamic Analysis was presented in the article *"Assessment of the seismic vulnerability of a reinforced concrete bridge using the Incremental Dynamic Analysis method"*, no. 166, January–February 2020, in collaboration with Prof. Dr. Eng. Răcănel Ionuț Radu.

SELECTIVE BIBLIOGRAPHY

[1] Radulian, M.; Popa, M.; Dinescu, R., "What we know and what we don't know about the earthquakes in the Vrancea region (Romania)," *Annals of the Academy of Romanian Scientists, Series on Physics and Chemistry Sciences,* Volume 8, Number 1/2023.

[2] Federal Emergency Management Agency, *FEMA 440: Improvement of Nonlinear Static Seismic Analysis Procedures,* Washington D.C., 2005.

[3] Federal Emergency Management Agency, *FEMA 356: Prestandard and commentary for the seismic rehabilitation of buildings,* Washington D.C., November 2000.

[4] Crețu, D., *Sisteme inovative pentru atenuarea efectului acțiunii seismice la structuri inginerești. Metoda izolării,* editura Conspress, 2015.

[5] EEFIT - Earthquake Engineering Field Investigation Team, *The Loma Prieta Earthquake of 17 October 1989,* Iulie 1993.

[6] Haiducu, A., "Reducerea efectului acțiunii seismice la structurile de poduri prin procedeul de izolare la nivelul de rezemare", Teză de Doctorat, București, 2012.

[7] Todd, D.; Carino, N.; Chung, R.M; Lew, H.S.; Taylor, A.W.; Walton, W.D.; Cooper, J.D.; Nimis, R., *1994 Northridge Earthquake: Performance of Structures, Lifelines, and Fire Protection Systems,* NIST Special Publication 862, Mai 1994.

[8] Chung, R., *The January 17, 1995 Hyogoken - Nanbu (Kobe) Earthquake,* NIST Special Publication 901, Iulie 1996.

[9] Sakellaridis, L.; Anastasopoulos, I.; Gazetas, G., *Fukae bridge collapse (Kobe 1995) revisited: New Insights,* Soils and Foundations, Volume 60, Issue 6, Decembrie 2020.

[10] Esper, P.; Tachibana, E., *Lessons from the Kobe earthquake,* Geological Society, London, October 1998.

[11] Elnashai, A.S; Gencturk, B.; Kwon, Oh-Sung; Al-Qadi, I.L.; Hashash, Y.; Roesler, J.R.; Kim, S.J.; Jeong, Seong-Hoon; Dukes, J.; Valdivia, A., *The Maule (Chile) Earthquake of February 27, 2010: Consequence Assesment and Case Studies,* MAE Center Report No. 10-04, Decembrie 2010.

[12] Scafati, F.; Ormando, C.; Clemente, P.; Buffarini G., *Seismic Isolation in Newly Built Bridges in Italy: Historical Development, Regulations, and Recent Applications,* BER - The International Journal of Bridge Engineering, Management and Research, October 2025.

[13] Roman, O.C.;, *Cercetări privind unele particularități ale proiectării geotehnice în condițiile seismice din zona Banat-Timișoara,* Teză de Doctorat, Timișoara, 2009.

[14] Șimon, V.;, *Descrierea acțiunii seismice în normele naționale, europene și internaționale. Modalități de descriere a acțiunii seismice,* Raportul de Cercetare Nr. 1, Ciclul Studii Doctorale, 2017.

[15] Constantinou, M.C.; Whittaker, A.S.; Fenz, D.M.; Apostolakis, G., *Seismic isolation of bridges,* pp. University at Buffalo, State University of New York, 30 Iunie 2007, Department of Civil, Structural and Environmental Engineering.

[16] Christopoulos, C.; Filiatrault, A., *Principles of Passive Supplemental Damping and Seismic Isolation,* Padova, Italia, 2006.

[17] Tensacciai, "Seismic Isolators," [Online]. Available: https://www.tensacciai.it/seismic-isolators.

[18] Freyssinet, "Earthquake protection devices ISOSISM range," [Online]. Available: https://www.freyssinet.co.nz/sites/default/files/earthquake_protection_devices_isosism.pdf.

[19] Robinson, W.H., *Lead-Rubber hysteretic bearings suitable for protecting structures during earthquakes,* Earthquake Engineering & Structural Dynamics: Volume 10, Issue 4, August 1982.

[20] Naeim, F.; Kelly, J.M., *Design of Seismic Isolated Structures: From Theory to Practice,* USA, 1999.

[21] Ucar, Y.; Altan, M.F., *Seismic Isolation Systems Against Earthquake Disaster,* Journal of Sustainable Construction Materials and Technologies, Mai 2018.

[22] Robinson, W.H., *Lead Rubber Hysteretic Bearings suitable for protecting structures during earthquakes,* The Journal of the Anti-Seismic Systems International Society (ASSIS), Vol. 2, No. 1, 2011.

[23] Cardone, D.; Gesualdi, G., "Restoring capability of friction pendulum seismic isolation systems," *Bulletin of Earthquake Engineering,* Ianuarie 2015.

[24] Briseghella, B.; Zordan, T.; Liu, T.; Mazzarolo, E., *Friction Pendulum System as a Retrofit Technique for Existing Reinforced Concrete Building,* Structural Engineering International, No. 2, 2013.

[25] Ponzo, F.C.; di Cesare, A.; Leccese, G.; Nigro, D., *Shake table testing on restoring capability of double concave friction pendulum seismic isolation systems,* Earthquake Engineering & Structural Dynamics, 2017.

[26] Petti, L.; Polichetti, F.; Lodato, A.; Palazzo, B., *Modelling and Analysis of Base Isolated Structures with Friction Pendulum System Considering near Fault Events,* Open Journal of Civil Engineering, 2013.

[27] FIP Industriale, "Curved Surface Sliders," [Online]. Available: https://www.fipmec.it/en/products/anti-seismic-devices/.

[28] Diotallevi, P.P.; Landi, L.; Grazi, G., *Modelling of friction pendulum isolators in structures subjected to horizontal and vertical ground motions,* Second European Conference on Earthquake Engineering and Seismology, Istanbul, 25-29 August, 2014.

[29] Popa, V., *P100 - 1/2013 - Cod de proiectare seismică - Partea I - Prevederi de proiectare pentru clădiri,* București, Mai 2013.

[30] Issa, M.; Issa, H., *Application of Pushover Analysis for the calculation of Behavior Factor for Reinforced Concrete Moment-Resisting Frames,* International Journal of Civil and Structural Engineering, Vol. 5, No. 3, 2015.

[31] Menon, A.; Magenes, G., *A review of the current status of seismic design and assessment of masonry buildings in Europe,* Journal of Structural Engineering (Madras), Februarie 2009.

[32] Vamvatsikos, D.; Cornell, C.A., "Incremental Dynamic Analysis," *Earthquake Engineering & Structural Dynamics,* vol. 31, no. 3, 2002.

[33] Computers & Structures, Inc., "Computers & Structures, Inc. - Structural and Earthquake Engineering Software," [Online]. Available: https://www.csiamerica.com/products/csibridge.

[34] Seismosoft, Earthquake Engineering Software Solutions, "SeismoArtif, SeismoMatch," [Online]. Available: https://seismosoft.com/.

[35] Șimon, V.M.; Răcănel, I.R., *Aprecierea vulnerabilității unui pod din beton armat la acțiunea seismică, utilizând metoda de Analiză Dinamică Incrementală,* Revista Construcțiilor, nr. 166, ianuarie-februarie 2020.